2008 IEEE International Conference on
Robotics and Automation
Pasadena, CA, USA, May 19-23, 2008

Workspace Characterization of a Robotic System Using Reliability-Based Design Optimization

Jeremy T. Newkirk, Alan P. Bowling and John E. Renaud

Abstract— **The workspace of a robotic system is characterized to determine the actuator inputs required to achieve a desired level of dynamic performance over a chosen percentage of configurations. The dynamic capability equations (DCE) allow designers to predict the dynamic performance of a robotic system for a particular configuration and reference point on the end-effector (i.e.,point design). Here the DCE are used in conjunction with a reliability-based design optimization (RBDO) strategy in order to obtain designs that can meet dynamic performance requirements. The method is illustrated on a robot design problem.**

I. Introduction

The focus of this study is to characterize the workspace, which is made up of all possible configurations, in an attempt to determine the actuator torques required to achieve a desired level of dynamic performance over a predetermined percentage of configurations. Most of the previous work done in this area attempted to find optimal path trajectories or optimal link sizes for specific path tracking, which include [1]–[4]. The work most similar to that presented here can be found in [5], but sampling of the workspace is required in order to complete the workspace characterization. The novelty of this work is the use of an optimization method for characterizing the workspace that does not require sampling in order to determine the size of the optimal actuators. The optimization used herein is reliability-based design optimization (RBDO).

The characterization of a robotic system presented in this work would allow a designer to be confident that the system would be able to achieve a desired level of dynamic performance over a desired range of configurations. For this work dynamic performance is defined as a manipulator's ability to accelerate its end-effector, *acceleration capability*, and to apply forces/moments to the environment at the end-effector, *force capability*. There are several dynamic performance measures and characterizations currently available in the literature including [6]–[9]. In this work, the *dynamic capability equations* (DCE) in [9] are used in conjunction with RBDO in order to obtain a more robust solution to the actuator selection problem. The characterization of the dynamic performance will be addressed.

Sampling techniques could be used to solve this problem, but they cannot take into account every possible configuration. RBDO is used in order to avoid statistical sampling and, since it is a gradient based method, is capable of taking into account all possible configurations. In this case the density functions allow for determination of the configuration with the highest probability of having the worst performance. This allows one to determine the probability that all configurations within the feasible region will yield some level of desired performance.

Reliability has often been associated with some type of failure in the robotic system and there is much recent work in this area. A popular area concerns addressing joint failure in robotic manipulators, in which the system actually malfunctions, from the standpoint of analysis [10], design [11], and control [12] and each of these papers references several other works on this topic. The failure model addressed by the proposed RBDO application is more concerned with not meeting performance goals rather than an actual malfunction of the system.

In the following sections previous work in the area of reliability methods is discussed first. The DCE and their use in the actuator selection problem are discussed next. This is followed by a discussion of reliability based optimization. Finally the method is applied to actuator selection for a two degree-of-freedom (DOF) planar manipulator.

II. Reliability Methods

There are a number of different reliability methods that have been applied to robotic systems. These methods include grey system theory, fuzzy Markov models and probabilistic approaches. Grey system theory is discussed in [14], Fuzzy Markov models are discussed in [15] and probabilistic approaches are discussed in [13], [16]. These reliability methods are used to determine the effects of errors due to manufacturing and controls on the reliability of the system. The application of RBDO, as discussed in this work, is to determine the probability that the system will be able to achieve a desired level of performance and at this stage does not take errors into account.

III. The DCE in Actuator Selection

Many different measures and characterizations of dynamic performance can be used as a basis for actuator selection including those proposed in [6]–[8], [17]–[19]. The DCE are used here because it is one of the few analyses that: 1) treats translational and rotational quantities in a consistent, physically-meaningful manner which satisfies *invariance to units and rotation* [20], [21], and 2) unifies the consideration of many different aspects of dynamic performance including accelerations, forces, and velocities. Few studies combine these quantities in their analyses excepting [8], [22] which consider accelerations and velocities, but do not address rotational and translational quantities.

The DCE are obtained from the equations of motion which can be expressed as

$$E(\bar{\mathbf{q}})\begin{bmatrix} \dot{\boldsymbol{v}} \\ \dot{\boldsymbol{\omega}} \end{bmatrix}+\mathcal{E}(\bar{\mathbf{q}})\begin{bmatrix} \mathbf{f} \\ \mathbf{m} \end{bmatrix}+\mathbf{C}(\dot{\mathbf{q}},\bar{\mathbf{q}},\boldsymbol{v},\boldsymbol{\omega})+\mathbf{g}(\bar{\mathbf{q}}) = \boldsymbol{\Upsilon} \quad (1)$$

where

$$\overline{\mathbf{q}}^T \;=\; \begin{bmatrix} \mathbf{q}^T & \mathbf{r}^T \end{bmatrix}^T \quad (2)$$

where $\mathbf{q} \in \mathbb{R}^{\mathbf{n}}$ contains the generalized coordinates and $\dot{\mathbf{q}}$ is its time derivative. The vectors $\boldsymbol{v}$ and $\boldsymbol{\omega}$, $[\boldsymbol{v}^T\ \boldsymbol{\omega}^T]^T \in \mathbb{R}^n$, are the translational and rotational velocities of the end-effector and $\dot{\boldsymbol{v}}$ and $\dot{\boldsymbol{\omega}}$ their time derivatives. The vectors $\mathbf{f}$ and $\mathbf{m}$, $[\mathbf{f}^T\ \mathbf{m}^T]^T \in \mathbb{R}^n$, are the contact forces at moments, and $\mathbf{g}(\mathbf{q}) \in \mathbb{R}^n$ and $\mathbf{C}(\dot{\mathbf{q}},\mathbf{q},\boldsymbol{v},\boldsymbol{\omega}) \in \mathbb{R}^n$ are the gravitational and *velocity* forces. The terms $E(\mathbf{q}) \in \mathbb{R}^{n\times n}$ and $\mathcal{E}(\mathbf{q}) \in \mathbb{R}^{n\times n}$ are the mass matrix and the transmission between end-effector and actuator forces.

The vector $\mathbf{r}$ in (2) represents the position of the operational point from a chosen reference point on the end-effector. It is assumed that $\mathbf{r}$ is a parameter in the problem which is specified. Note that $\boldsymbol{v}$ and $\boldsymbol{\omega}$ are the velocities of the point specified by $\mathbf{r}$ and the rotation of the end-effector about the point defined by $\mathbf{r}$. This vector represents the variability of the operational point.

The bounds on actuator torque, $\boldsymbol{\Upsilon}_{bound}$, are expressed as

$$-\boldsymbol{\Upsilon}_{bound} \;\le\; \boldsymbol{\Upsilon} \;\le\; \boldsymbol{\Upsilon}_{bound} \quad (3)$$

The idea here is to compare the actuator torques required to produce balanced acceleration and force capabilities, to the total available actuator torques defined by the bounds in (3). This is done by specifying all of the terms on the left-hand-side of (1), including the configuration $\mathbf{q}$ and operational point $\mathbf{r}$, and determining the torque required to produce those specified motions. The dynamic capabilities are specified in a manner that allows each constraint to maintain homogeneous units

$$\begin{array}{rclrcl} \dot{\boldsymbol{v}}^T\dot{\boldsymbol{v}} &=& |\dot{v}|^2 & \dot{\boldsymbol{\omega}}^T\dot{\boldsymbol{\omega}} &=& |\dot{\omega}|^2 \\ \boldsymbol{v}^T\boldsymbol{v} &=& |v|^2 & \boldsymbol{\omega}^T\boldsymbol{\omega} &=& |\omega|^2 \\ \mathbf{f}^T\mathbf{f} &=& |\mathrm{f}|^2 & \mathbf{m}^T\mathbf{m} &=& |\mathrm{m}|^2 \end{array} \quad (4)$$

where $|\dot{v}|$ represents the *balanced translational acceleration*, which bounds the magnitude $\|\dot{\boldsymbol{v}}\|$, and likewise for the other balanced quantities. *In general, each relation represents a sphere.*

Omitting the details, the performance of the robot is described by the DCE expressed as

$$\mathbb{A}\begin{bmatrix} |\dot{v}| \\ |\dot{\omega}| \end{bmatrix} \;+\; \mathbb{C}\left(|v|^2,|\omega|^2\right) \;+\; \mathbb{F}\begin{bmatrix} |\mathrm{f}| \\ |\mathrm{m}| \end{bmatrix} \;\le\; \mathbb{T} \quad (5)$$

where

$$\mathbb{T} \;=\; \begin{bmatrix} \boldsymbol{\Upsilon}_{bound} \\ \boldsymbol{\Upsilon}_{bound} \end{bmatrix} - \mathbb{G} \quad (6)$$

and where $\mathbb{A}$, $\mathbb{C}$, $\mathbb{F}$, $\mathbb{G}$, and $\mathbb{T}$ are derived from E, $\mathbf{C}$, $\mathcal{E}$, $\mathbf{g}$, and $\boldsymbol{\Upsilon}_{bound}$; see [9], [23]. The largest possible values of the balanced quantities in the DCE define what is referred to as the dynamic capability hypersurface (DCH). Since the six-dimensional hypersurface is difficult to visualize, three-dimensional sections of it are examined in order to investigate its properties. A section of the hypersurface, where $|\omega| = |\mathrm{f}| = |\mathrm{m}| = 0$, is shown in Fig. 1a for the PUMA 560 manipulator, at the configuration shown in Fig. 1b. Notice in Fig. 1a that the balanced accelerations go to zero as velocity increases.

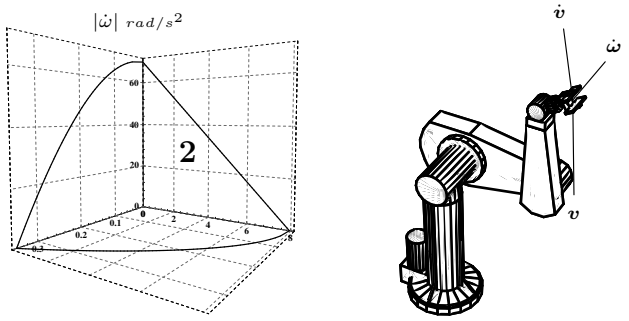

(a) (b)

Fig. 1. PUMA 560 Dynamic Capability Hypersurface Sections.

The DCE actually describe the worst-case combinations of acceleration, velocity, and force which saturate at least one actuator, referred to as *worst-case motions/forces*. The saturated actuator, referred to as the *limiting actuator*, is indicated by the numeric label on the surface of Fig. 1a. The *worst-case directions of motion* that caused the particular actuator to saturate are indicated by the line segments emanating from the end-effector of the PUMA 560 in Fig. 1b.

The DCE and DCH describe the robot's dynamic performance given a set of actuator torques. The inverse problem is to specify a desired dynamic performance and to determine the actuator torques that will provide that level of performance. This is the actuator selection problem discussed in [5], [23], [24]. The desired performance is specified by describing the desired shape of the DCH using performance points of the form

$$p_i = (\ |\dot{v}|_i,\ |\dot{\omega}|_i,\ |\mathrm{f}|_i,\ |\mathrm{m}|_i,\ |v|_i,\ |\omega|_i\ ) \quad (7)$$

where $i = 1,\ldots,n$ and each i refers to an individual performance point. Actuators are then chosen such that the DCH encompasses all of the performance points.

The basic idea is to substitute these points into the DCE in order to determine whether the specified performance is feasible or not. These relations act as constraints on an optimization problem; see [5], [24]. The optimization

problem is

$$\begin{aligned}
\min_{\boldsymbol{\Upsilon}_{bound},\ \alpha_i} \quad & \text{cost} = \tfrac{\Upsilon_{bound_1}}{\Upsilon_{min_1}} + \cdots + \tfrac{\Upsilon_{bound_n}}{\Upsilon_{min_n}} \\
\text{s.t.} \quad & \boldsymbol{\Upsilon}_{min} \le \boldsymbol{\Upsilon}_{bound} \le \boldsymbol{\Upsilon}_{max} \\
& \alpha_i \ge 1 \\
& g_i^R = \alpha_i \, \mathbb{A} \begin{bmatrix} |\dot{v}|_i \\ |\dot{\omega}|_i \end{bmatrix} + \alpha_i^2 \, \mathbb{C} \left(|v|_i^2, |\omega|_i^2 \right) + \\
& \alpha_i \, \mathbb{F} \begin{bmatrix} |\mathrm{f}|_i \\ |\mathrm{m}|_i \end{bmatrix} + \mathbb{G} - \begin{bmatrix} \boldsymbol{\Upsilon}_{bound} \\ \boldsymbol{\Upsilon}_{bound} \end{bmatrix} \le 0
\end{aligned} \tag{8}$$

where $i = 1, \ldots, p$ and p is the number of performance points, $\boldsymbol{\Upsilon}_{min}$ and $\boldsymbol{\Upsilon}_{max}$ are the minimum and maximum achievable torques and α_i is a weighting factor for the DCE constraint. The objective in (8) is to find the optimum values of the motor torques and the scalars α_i that minimize the weighted sum of torques and satisfy the performance constraints g_i^R.

Herein, the deterministic optimization problem in (8) is transformed into an RBDO problem. The RBDO approach is used to select actuators taking into account all possible configurations of the system with a fixed operational point. The RBDO finds actuators that will satisfy the performance constraints to within a certain *probability of failure*. Inability to achieve the performance point is the dominant *failure mode* in actuator selection. These concepts are discussed next in Sec. IV.

IV. Reliability-Based Design Optimization

The dynamic performance characterization over the configuration space can be addressed statistically by sampling a number of configurations. However, it is desirable to address this problem without sampling. The RBDO approach can achieve this over a configuration space that does not contain singularities. Thus this technique is well-suited for addressing this issue.

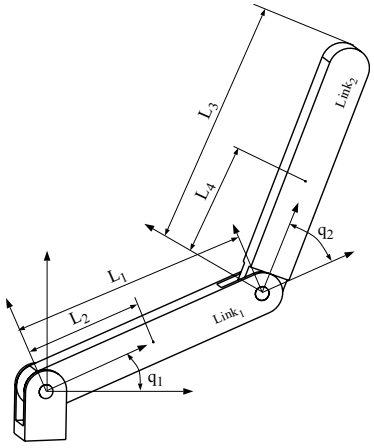

Fig. 2. Two DOF Robot.

Here a simple example, the two DOF planar manipulator shown in Fig. 2, is used to illustrate the RBDO approach. The end effector is assumed to be located at the end of link 2. A feasible range of configurations can be defined as $0^\circ \le q_1 \le 180^\circ$ and $-90^\circ \le q_2 \le 0^\circ$ for example.

A. Most Probable Point (MPP) of Failure

The RBDO approach relies on finding the *most probable point* (MPP) of failure, the point $({q_1}_i{}^*, {q_2}_i{}^*)$ within the feasible region most likely to violate the performance constraint g_i^R in (8). It is analogous to the worst-case motions/forces which define the DCH discussed in Sec. III.

In (4) the accelerations, velocities, and forces were specified in terms of their magnitudes which allowed for determination of worst-case performance. This was possible because the equations of motion are linear with respect to accelerations and forces, and purely quadratic with respect to velocities. The dynamic model and the resulting DCE are highly nonlinear with respect to the configuration $\mathbf{q}$, which appears as an argument to transcendental functions. For this problem q_1 and q_2 are considered as variables, so the dynamic model is nonlinear with respect to the variables. Yet specifications for q_1 and q_2, which allow for analysis of worst-case performance in terms of the MPP, can be developed using *probability density functions* (PDF).

There are several methods for estimating the MPP such as the first and second order reliability methods, (FORM) and (SORM) [25], [26]. These methods reduce the computational time required to solve for the optimal solution. An efficient and robust method using Taylor series expansion and gradients is explained in [27]. Here the details of these methods are omitted, but the following discussion explains their underlying concepts.

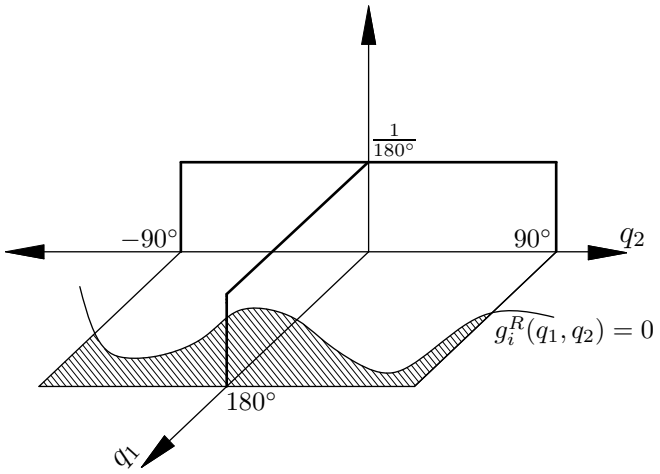

Fig. 3. Uniform PDFs for q_1 and q_2.

There is no preferred configuration, so the parameters q_1 and q_2 are specified as random variables having uniform PDFs as shown in Fig. 3. The goal here is to determine the *probability of failure*, P_{f_i},

$$P_{f_i} = \int_{g_i^R(q_1,q_2) \ge 0} f(q_1, q_2) \, dq_1 \, dq_2 \tag{9}$$

that the ith performance constraint will be violated. This is found by integrating the joint PDF, $f(q_1, q_2)$, over the failure domain $g_i^R(q_1, q_2) \geq 0$, represented by the hatched region in Fig. 3. However, the joint PDF $f(q_1, q_2)$ is nearly impossible to find for random variables [25]. One must evaluate g_i^R at several sample points in the feasible region, yielding a discrete joint PDF, to determine $f(q_1, q_2)$ with any surety; however, here the effort is to avoid sampling.

The integral in (9) can be approximated using the FORM [25]. This technique uses a change of variables from the uniform PDFs shown in Fig. 3 to standard normal PDFs

$$\begin{aligned} q_{1i}(u_{q_{1_i}}) &= 180^\circ \ \Phi(u_{q_{1_i}}) \\ q_{2i}(u_{q_{2_i}}) &= -90^\circ + 90^\circ \ \Phi(u_{q_{2_i}}) \end{aligned} \tag{10}$$

where

$$\Phi(u) = \int_{-\infty}^{u} N(u) \ du \tag{11}$$

and where $N(u)$ is a standard normal or Gaussian PDF with a zero mean and $-\infty \leq u \leq \infty$. Realize that $0 \leq \Phi(u) \leq 1$ in (10), thus the range of $\Phi(u)$ covers the feasible range of q_1 and q_2. Also note that with this change of variables the performance constraints can be expressed as

$$G_i^R(u_{q_{1_i}}, u_{q_{2_i}}) = g_i^R \left(q_{1i}(u_{q_{1_i}}), q_{2i}(u_{q_{2_i}}) \right) \ . \tag{12}$$

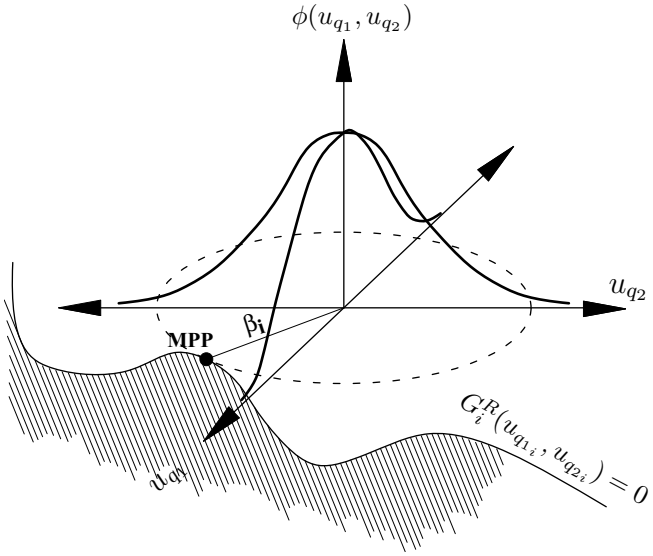

Fig. 4. Standard Normal Joint PDF $\phi(u_{q_1}, u_{q_2})$.

The FORM version of the MPP is obtained as the solution to an optimization problem referred to as the *Performance Measure Approach* (PMA) [28], [29]

$$\begin{aligned} \min_{u_{q_{1_i}},\ u_{q_{2_i}}} \quad & \text{cost} = G_i^R(u_{q_{1_i}}, u_{q_{2_i}}) \\ \text{subject to} \quad & \mathbf{u}_i^T \mathbf{u}_i = \beta_i^2 \quad \text{where} \quad \mathbf{u}_i = \begin{bmatrix} u_{q_{1_i}} \\ u_{q_{2_i}} \end{bmatrix} \end{aligned}$$

where the value of the *reliability index* β_i determines the probability that the ith performance constraint is satisfied. The solution, $(\mathbf{u}_i^*)^T = \begin{bmatrix} u_{q_{1_i}}^* & u_{q_{2_i}}^* \end{bmatrix}^T$, is used to find the MPP in terms of $q_{1_i}^*(u_{q_{1_i}}^*)$ and $q_{2_i}^*(u_{q_{2_i}}^*)$. An estimate of P_{f_i} in (9) can be found as:

$$\begin{aligned} P_{f_i} &= \int_{G_i^R(u_{q_{1_i}}, u_{q_{2_i}}) \geq 0} \phi(u_{q_1}, u_{q_2}) \ du_{q_1} \ du_{q_2} \\ &\approx 1 - \Phi(\beta_i) = P_{allow_i} \end{aligned} \tag{13}$$

where the composition of $\phi(u_{q_1}, u_{q_2})$ and the distance β_i are shown in Fig. 4. The function Φ is defined in (11) and its use in (14) is discussed in [25]. The volume beneath $\phi(u_{q_1}, u_{q_2})$ bounded by the dashed circle shown in Fig. 4 is $\Phi(\beta_i)$ which is subtracted from the total volume beneath $\phi(u_{q_1}, u_{q_2})$, 1, yielding the estimate of P_{f_i} given in (14). It is an estimate because the domain defined by $1 - \Phi(\beta_i)$ can be larger/smaller than that defined by $G_i^R(u_{q_{1_i}}, u_{q_{2_i}}) \geq 0$, shown as the hatched region in Fig. 4. Note that this estimate is obtained without sampling the feasible region of q_1 and q_2 shown in Fig. 3. The *allowable probability of failure*, P_{allow_i}, is determined by the choice of β_i.

The assumption that q_1 and q_2 are random variables with uniform probability distributions may not be entirely correct, but this assumption greatly simplifies the problem presented here and does not affect the goal of this research. The goal here is to determine the feasibility of applying RBDO to a robotic system. An approach for solving RBDO problems with uncertain probability distributions is presented in [30].

B. RBDO

The RBDO version of (8) is expressed as

$$\begin{aligned} \min_{\boldsymbol{\Upsilon}_{bound}\ \alpha_i} \quad & \text{cost} = \frac{\Upsilon_{bound_1}}{\Upsilon_{min_1}} + \cdots + \frac{\Upsilon_{bound_n}}{\Upsilon_{min_n}} \\ \text{subject to} \quad & \boldsymbol{\Upsilon}_{min} \leq \boldsymbol{\Upsilon}_{bound} \leq \boldsymbol{\Upsilon}_{max} \\ & \alpha_i \geq 1 \\ & G_i^R(\mathbf{u}_i^*) \leq 0 \end{aligned} \tag{14}$$

where the performance constraints represented by G_i^R are evaluated at the MPP found in (13).

The formulation in (14) involves a sub-optimization, the problem in (13), which must be solved at each iteration. This is computationally inefficient and therefore a unilevel optimization problem has been formulated. The concepts underlying the unilevel method are the same as those for (14) so it will not be discussed in detail; see [27]. However, the unilevel approach is used in the example presented in Sec. V and it is expressed as:

$$\begin{aligned} \min_{\boldsymbol{\Upsilon}_{bound},\ \alpha_i,\ \mathbf{u}_i} \quad & \text{cost} = \frac{\Upsilon_{bound_1}}{\Upsilon_{min_1}} + \frac{\Upsilon_{bound_2}}{\Upsilon_{min_2}} \qquad (15) \\ \text{subject to} \quad & \boldsymbol{\Upsilon}_{min} \leq \boldsymbol{\Upsilon}_{bound} \leq \boldsymbol{\Upsilon}_{max} \\ & \alpha_i \geq 1 \\ & G_i^R(\mathbf{u}_i) \leq 0 \\ & \mathbf{u}_i^T \mathbf{u}_i = \beta_i^2 \qquad (16) \\ & h_{1_i}(u_{q_{1_i}}, u_{q_{2_i}}) = 0 \qquad (17) \end{aligned}$$

where

$$h_{1_i}(u_{q_{1_i}}, u_{q_{2_i}}) \equiv \|\mathbf{u}_i\| \ \|\nabla_{\mathbf{u}} G_i^R\| + \mathbf{u}_i^T \nabla_{\mathbf{u}} G_i^R \ . \tag{18}$$

In the unilevel RBDO, the constraint from (13) is added to the main problem as (16), and the minimization of the cost function in (13) is replaced by the corresponding first order necessary Karush-Kuhn-Tucker optimality conditions in (18). The RBDO problem developed in this section for the example in Fig. 2 can easily be generalized.

Other methods such as Sequential Optimization and Reliability Assessment (SORA) can also be used to reduce problems such as the one presented here to a unilevel problem. The details for SORA are presented in [31], [32]. However, the SORA method solves the deterministic optimization problem and then applies a reliability assessment. The desire to avoid the sampling of the design space required with use of the deterministic optimization, due to the highly nonlinear nature of the problem, makes the SORA method less attractive for this application.

V. Example

Here the unilevel RBDO is performed on the two DOF planar manipulator shown in Fig. 2, using the theory developed in Sec. IV. The dynamic model parameters are the link lengths, link masses, and moments of inertia which are given in Table Ic. The desired level of performance, see (7), is specified as

$$p_1 \;=\; (\; 9.8\ m/s^2,\; 0,\; 0,\; 0,\; 0,\; 0\;)\;. \tag{19}$$

The parameters for the RBDO are given in Table Ib. Three different allowable failure probabilities were used to test this method for varying degrees of reliability. The allowable failure probability of 0.0013, which corresponds to a desired reliability index of 3 is a strong requirement stating that 99.87% of all configurations in the feasible range, given in Table Ia, will satisfy the performance point p_1. Similarly, the reliability indices 1 and 2 correspond to 84.13% and 97.72% of configurations satisfying the performance point p_1.

TABLE I
RBDO Optimization Data for the Configuration Space.

a.) Statistics for the Random Variables		
	Distribution	Range
q_1	Uniform	$0^\circ \le q_1 \le 180^\circ$
q_2	Uniform	$-90^\circ \le q_2 \le 0^\circ$
b.) RBDO Optimization Parameters		
	β_1	P_{allow_1}
	1	0.1587
	2	0.0228
	3	0.0013
c.) Parameters for the Actuator Selection		
	Link 1	Link 2
Mass kg	1	1
Length m	0.3048	0.3048
Inertia kgm^2	0.001	0.001

The ranges for q_1 and q_2 are shown in Table Ia. A singularity occurs when q_2 is at 0°, so that is the reason for the chosen range. The variable q_2 is allowed to range up to the singularity, but is not allowed to pass through it. Singularities are a cause of concern in gradient based optimization methods. This is due to the fact that these methods use the derivative of the original function to find the direction of steepest ascent or descent. At singular points the derivative goes to infinity, so a steepest ascent or descent direction does not exist. Therefore, these methods are not able to find extremum points, or points where the derivative goes to zero, since it continues to search at the location of the singularity. For this reason singular configurations were avoided in this example, but singularity avoidance methods are discussed at the end of this chapter.

The purpose of this example is to show that RBDO can be used to characterize the dynamic performance of a robotic system over all possible configurations without having to resort to sampling methods. This ensures that all possible configurations of the system are taken into account. The goal of this is to find actuators that will produce a desired level of performance over a desired percentage of configurations. If no singularities are present in the system it is possible to find actuators that will provide a desired level of performance over the entire configuration space. Due to the singularity in this example it is only possible to provide a desired level of performance over almost all configurations.

Table II shows results obtained for the RBDO method using the three beta values. The effects on dynamic performance of a change in configuration can be highly nonlinear so it was necessary to compare the results with the corresponding reliability values obtained from a monte carlo simulation. The monte carlo simulation sampled 100,000 points in the configuration space using the optimal actuator torques obtained from the RBDO method shown in Table II.

TABLE II
RBDO Optimization Data for Variable Configurations.

Results of RBDO					
β	$\Upsilon_{bound_1}\ Nm$	$\Upsilon_{bound_2}\ Nm$	α_1	Des. Rel.	M.C. Rel.
1	18.59	3.66	1	84.13%	86.19%
2	89.66	15.45	1	97.72%	97.85%
3	1414.70	236.28	1	99.87%	99.88%

The results show that the method works very well when compared with a monte carlo simulation. The results are especially close for very high reliability values. The fact that an approximate method, namely FORM, is used in the optimization explains the loss of accuracy with lower reliability values. However, even those results are very close to the values obtained through the monte carlo method.

For this simple example the singularity could be avoided by limiting the range of q_2 without loss of information about the system due to the symmetry from one side of the singularity to the other. The location of the singularity was also easily determined, however for a more complex system it may not be as easy to locate the singularity and

if it can be located limiting the range of a joint variable may cause loss of information. Some performance measure approaches have been proposed, which are used to avoid singularities and may provide solutions that do not cause a loss of information. These methods include singular value decomposition, manipulability and condition number. These methods are discussed in [33]. These performance index methods are all used to locate singularities for the purpose of avoiding these locations, but the application of RBDO to determine the dynamic performance of a system needs to take these singularities into account. These methods could likely be used with the RBDO method to locate singularities and account for them in order to avoid failure of the optimization.

VI. Conclusions

This investigation focuses on improving the design and reliability of robotic systems by characterizing the workspace. Implementation of a novel unilevel approach for RBDO facilitates the improved design of robotic systems which can more reliably achieve their desired performance level. This RBDO method eliminates the need to sample the workspace, therefore it is a robust method for characterizing the workspace of the robotic system. The unilevel RBDO approach for robotic system design will have a significant impact in applications where a high level of performance is critical, such as site cleanup where failure or inability of the robot to handle a toxic payload may result in spillage, which could be catastrophic for the environment.

References

[1] Z. Shiller and S. Sundar, "Design of robotic manipulators for optimal dynamic performance," in *Proceedings of the 1991 International Conference on Robotics and Automation*, April 1991, pp. 344–349, sacramento, CA.

[2] ——, "Manipulator design for optimal dynamic motions along specified paths," in *Proceedings of the American Control Conference*, vol. 2, 1991, pp. 2033–2038.

[3] K. G. Shin and N. D. McKay, "Dynamic programming approach to trajectory planning of robotic manipulators," in *IEEE Transactions on Automatic Control*, vol. AC-31, 1986, pp. 491–500.

[4] C. haur Wu and C. cheng Jou, "A study on the movement capability of robot manipulators," in *Proceeding of the 28th Conference on Decision and Control*, vol. December, 1989, pp. 2500–2505.

[5] A. Bowling and O. Khatib, "Actuator selection for desired dynamic performance," in *Proceedings of the IEEE/RSJ International Conference on Intelligent Robots and Systems*, vol. 2, October 2002, pp. 1966–1973, Lausanne, Switzerland.

[6] T. Yoshikawa, "Dynamic manipulability of robot manipulators," in *Proceedings IEEE International Conference on Robotics and Automation*, 1985, pp. 1033–1038, St. Louis, Missouri, USA.

[7] T. J. Graettinger and B. H. Krogh, "The acceleration radius: A global performance measure for robotic manipulators," *IEEE Journal of Robotics and Automation*, vol. 4, no. 1, pp. 60–69, February 1988.

[8] Y. Kim and S. Desa, "The definition, determination, and characterization of acceleration sets for spatial manipulators," *The International Journal of Robotics Research*, vol. 12, no. 6, pp. 572–587, 1993.

[9] A. Bowling and O. Khatib, "The dynamic capability equations: A new tool for analyzing manipulator dynamic performance," *IEEE Transactions on Robotics*, vol. 21, no. 1, pp. 115–123, February 2005.

[10] R. G. Roberts and A. A. Maciejewski, "A local measure of fault tolerance for kinematically redundant manipulators," *IEEE Transactions on Robotics and Automation*, vol. 12, no. 4, pp. 543–552, August 1996.

[11] M. Hassan and L. Notash, "Design modification of parallel manipulators for optimum fault tolerance to joint jam," *Mechanism and Machine Theory*, vol. 40, no. 5, pp. 559–577, May 2005.

[12] C. Bonivento, L. Gentili, and A. Paoli, "Internal model based fault tolerant control of a robot manipulator," in *Proceedings of the IEEE Conference on Decision and Control*, vol. 5, 2004, pp. 5260–5265.

[13] P. K. Bhatti and S. S. Rao, "Reliability analysis of robot manipulators," *Journal of Mechanisms, Transmissions, and Automation in Design*, vol. 110, no. 2, pp. 175–181, June 1988.

[14] M. Y. Ming, J. G. Chao, and A. Y. Chen, "Analysis of manipulator movement reliability," in *Proceedings 2nd Asian Conference on Robotics and Its Applications*, October 1994, pp. 195–199.

[15] M. Leuschen, I. Walker, and J. Cavallaro, "Robot reliability through fuzzy markov models," in *Annual Reliability and Maintainability Symposium 1998 Proceedings*, January 1998, pp. 209–214.

[16] Z. Shi, "Reliability analysis and synthesis of robot manipulators," in *Proceedings of Annual Reliability and Maintainability Symposium*, January 1994, pp. 201–205.

[17] O. Khatib and S. Agrawal, "Isotropic and uniform inertial and acceleration characteristics: Issues in the design of redundant manipulators," in *Proceedings of the IUTAM/IFAC Symposium on Dynamics of Controlled Mechanical Systems*, 1989, Zurich, Switzerland.

[18] P. Chiacchio, S. Chiaverini, L. Sciavicco, and B. Siciliano, "Reformulation of dynamic manipulability ellipsoid for robotic manipulators," in *Proceedings IEEE International Conference on Robotics and Automation*, vol. 3, 1991, pp. 2192–2197, Sacramento, California, USA.

[19] P. Chiacchio, "A new dynamic manipulability ellipsoid for redundant manipulators," *Robotica*, vol. 18, pp. 381–387, 2000.

[20] K. L. Doty, C. Melchiorri, E. M. Schwartz, and C. Bonivento, "Robot manipulability," *IEEE Transactions on Robotics and Automation*, vol. 11, no. 3, pp. 462–468, 1995.

[21] K. Kazerounian and J. Rastegar, "Object norms: A class of coordinate and metric independent norms for displacements," *Flexible Mechanisms, Dynamics, and Analysis*, vol. 47, pp. 271–275, 1992.

[22] J. V. et. al, "Contribution to analyse manipulator morphology coverage and dexterity," in *Proceedings of the First CISM-IFToMM Symposium on Theory and Practice of Robots and Manipulators (Romansy 1)*. Springer-Verlag, September 1973, pp. 277–302, kupari, Yugoslavia.

[23] A. Bowling and C. Kim, "Velocity effects on robotic manipulator dynamic performance," *ASME Journal of Mechanical Design*, 2006, In press.

[24] A. Bowling and O. Khatib, "The dynamic loading criteria in actuator selection for desired dynamic performance," *Advanced Robotics*, vol. 17, no. 7, pp. 641–656, November 2003.

[25] A. Haldar and S. Mahadevan, *Probability, Reliability and Statistical Methods in Engineering Design*. John Wiley & Sons, 2000.

[26] A. Chiralaksanakul and S. Mahadevan, "First-order approximation methods in reliability-based design optimization," *Journal of Mechanical Design*, vol. 127, no. 5, pp. 851–857, 2005.

[27] H. Agarwal and J. E. Renaud, "A unilevel method for reliability based design optimization," in *Proceedings of the 45rd AIAA/ASME/ASCE/AHS/ASC Structures, Structural Dynamics, and Materials Conference*. AIAA-2004-2029, Palm Springs, CA. April 19-22 2004.

[28] K. K. Choi, B. D. Youn, and R. Yang, "Moving least square method for reliability-based design optimization," in *Proceedings of the Fourth World Congress of Structural and Multidisciplinary Optimization*, Dalian, China, June 4-8, 2001 2001.

[29] B. D. Youn and K. K. Choi, "An investigation of nonlinearity of reliability-based design optimization approaches," *Journal of Mechanical Design*, vol. 126, no. 3, pp. 403–411, 2004.

[30] X. Du, A. Sudjianto, and B. Huang, "Reliability-based design with the mixture of random and interval variables," *Journal of Mechanical Design*, vol. 127, no. 6, pp. 1068–1076, 2005.

[31] X. Du and W. Chen, "Sequential optimization and reliability assessment method for efficient probabilistic design," *Journal of Mechanical Design*, vol. 126, no. 2, pp. 225–233, 2004.

[32] X. Du, A. Sudjianto, and W. Chen, "An integrated framework for optimization under uncertainty using inverse reliability strategy," *Journal of Mechanical Design*, vol. 126, no. 4, pp. 562–570, 2004.

[33] T. Tanev and B. Stoyanov, "On the performance indexes for robot manipulators," *Problems of Engineering Cybernetics and Robotics*, vol. 49, pp. 64–71, 2000.